Applied Scientific Research 44: 197–207 (1987)

Mathematical modelling of bubble driven flows in metallurgical processes

S.T. JOHANSEN [1], F. BOYSAN [2] & W.H. AYERS [2]
[1] *Norwegian Institute of Technology, Department of Metallurgy, Trondheim, Norway;*
[2] *University of Sheffield, Department of Chemical Engineering and Fuel Technology, Sheffield S1 3JD, UK*

Abstract. The complex fluid dynamics of two-phase bubbly flows in metallurgical reactors is modelled numerically by using a $k-e$ turbulence model for the liquid phase, with a driving force determined by considering the motion of the bubbles. The latter are affected by the buoyancy forces and the drag caused by their relative motion with the mean and turbulent motions of the liquid, the turbulent component being obtained by random sampling to give an ensemble of bubble trajectories. The two-way coupling between the two phases is resolved by an iterative procedure which converges on a stable overall solution. The results are compared with measurements carried out on an air–water model and show good overall agreement.

Introduction

In recent years, gas-stirring in metallurgical reactions has become increasingly popular due to its effectiveness and low cost. The gas can be introduced into a bath of molten metal either through porous plugs, or using nozzles or lances. For flow rates below 300 kg/m^2-s and bottom injection, the resulting flow field is classified as a bubbling jet [1]. In this flow regime, large unstable bubbles break up into smaller ones shortly after detachment leading to a plume-like two-phase flow region with high voidage. The bubbles which rise due to gravity exchange momentum with their surroundings, which in turn induce a large toroidal vortex in the melt due to the confinement of the flow.

The metallurgical events which then take place in the reactor are largely governed by the velocity and turbulence fields. This is exemplified by the deposition and re-entrainment of inclusions, as well as refractory wear, which are controlled by the fluid dynamics, while homogenization and chemical reaction rates depend on the structure of turbulence. In circumstances where the reactor is operated on a continuous basis, the performance is governed by the degree of stirring, agitation and residence time. Short-circuiting is therefore to be avoided when dissolved species are to be removed from the melt by inert gas injection. When bubbles contain reactive gases, it is important to avoid high local void fractions otherwise chemical equilibrium is difficult to attain and gas is wasted.

In spite of the important role that the fluid dynamics plays in gas-stirred reactors, the analysis of the two-phase flow field from first principles has so far been only partially successful. Previous studies on this subject have mainly

been directed towards obtaining the field distributions of velocity components and turbulence quantities in the melt without attempting to model the two-phase region. Szekely et al. [2] have assumed that the bubble column was cylindrical in shape and imposed measured values of velocities as boundary conditions on its periphery. Although the authors could obtain reasonable qualitative agreement between the calculations and the measured data, unsatisfactory quantitative agreement was reported. The importance of the void fraction distribution in the two-phase region in the prediction of the melt velocity distributions has been emphasized in recent studies by Guthrie and co-workers [3], who developed an elaborate phenomenological model of the bubble column, and by He Qinglin et al. [4] who used the measured void fraction and inter-phase force distributions in the governing equations of the conservation of mass and momentum in the liquid phase.

Although semi-empirical models of the two-phase region can lead to reliable predictions of the flow field in the melt for a given configuration and operating conditions, such models conspicuously lack generality and hence cannot be used to analyse a new configuration or operating point with any confidence. The key to the development of a general model of gas-stirring therefore lies in a detailed representation of the motion of the gas bubbles and their interaction with the liquid phase.

The present study addresses itself to the development of such a mathematical model, which differs from earlier contributions in attempting to model the motion of the bubbles, as well as that of the liquid, from first principles. The sets of partial differential equations so obtained are solved numerically using a minicomputer, and the results of these calculations are compared with both axisymmetric and asymmetric bubble jet configurations which have been studied experimentally.

Liquid phase equations

The equations which describe the motion of the liquid phase are the time averaged balances of mass and momentum which will be given here in compact tensor notation for brevity.

Continuity

$$\frac{\partial}{\partial x_i}\alpha_l \rho_l u_i = 0. \tag{1}$$

Momentum conservation

$$\frac{\partial}{\partial x_i}\alpha_l \rho_l u_i u_j = -\alpha_l \frac{\partial p}{\partial x_j} + \frac{\partial}{\partial x_i}\alpha_l \mu_l \left(\frac{\partial u_i}{\partial x_j} + \frac{\partial u_j}{\partial x_i} \right) - \frac{\partial}{\partial x_i}\alpha_l \rho_l \langle u_i' u_j' \rangle + F_j. \tag{2}$$

Where, u_j and u_j' are the mean and fluctuating parts of the velocity component in the direction x_j, p is the pressure, ρ_l is the density, μ_l is the viscosity and α_l is the liquid volume fraction. The j-component of momentum exchange between the gas and the liquid is contained in the term F_j. These equations are obtained from the Navier-Stokes equations by velocity decomposition and time averaging (denoted by angled brackets) assuming that the fluctuations in volume fraction can be neglected. They cannot be solved (numberically or otherwise) unless the pair correlations of the fluctuations are related to known or calculable quantities by a turbulence model, and the distribution of the inter-phase force F_j is provided in some way.

Many models of turbulence of varying complexity have been proposed in the past which range from the simple mixing length model to more sophisticated second order closures and large eddy simulations. The widely used k–ϵ model [5] provides a compromise between these two extremes which uses as its starting point a Boussinesq type of relationship between the Reynolds stresses and the rate of mean strain:

$$\rho_l \langle u_i' u_j' \rangle = \tfrac{2}{3}\rho_l k \delta_{ij} - \mu_t \left(\frac{\partial u_i}{\partial x_1} + \frac{\partial u_j}{\partial x_i} \right). \tag{3}$$

Where k is the kinetic energy of the fluctuating motion, μ_t is a turbulent viscosity which is a property of the particular flow situation rather than of the fluid and δ is the kronecker delta. The spatial distribution of μ_t is related to the kinetic energy of turbulence k and its rate of dissipation ϵ through

$$\mu_t = \rho_l C_\mu \frac{k^2}{\epsilon}. \tag{4}$$

Where C_μ is a constant. The fields of k and ϵ are provided by the solution of the following transport equations:

$$\frac{\partial}{\partial x_i} \alpha_l \rho_l u_i k = \frac{\partial}{\partial x_i} \alpha_l \mu_t \frac{\partial k}{\partial x_i} + \alpha_l \rho_l \left(- \langle u_i' u_j' \rangle \frac{\partial u_i}{\partial x_i} - \epsilon \right) \tag{5}$$

and

$$\frac{\partial}{\partial x_i} \alpha_l \rho_l u_i \epsilon = \frac{\partial}{\partial x_i} \alpha_l \frac{\mu_t}{\sigma_\epsilon} \frac{\partial \epsilon}{\partial x_i} + \alpha_l \rho_l \left(- C_1 \langle u_i' u_j' \rangle \frac{\partial u_i}{\partial x_j} - C_2 \frac{\epsilon^2}{k} \right). \tag{6}$$

Where the constants C_μ, C_1 and C_2 and σ_ϵ are given the values

$$C_\mu = 0.09, \quad C_1 = 1.44, \quad C = 1.92 \quad \text{and} \quad \sigma_\epsilon = 1.3.$$

The above model is probably only a crude approximation to bubbly flow because the turbulence is scaled on the gradients of the mean flow rather than on the bubble size, and is employed here in the absence of anything more suitable.

The motion of the gas bubbles

Two different approaches are currently available for the analysis of the behaviour of a dispersed phase in turbulent flows. These are termed the continuum (Eulerian) and discrete (Lagrangian) methods. In the continuum approach the problem is formulated in terms of mass and momentum conservation equations for each phase in an Eulerian reference frame. In the discrete method on the other hand, the trajectories of individual bubbles are tracked in time by solving ordinary differential equations and the momentum interchange between the phase is accounted for by recording what is gained or lost by the bubbles as they pass through the liquid and using this information in the equations of the continuous phase.

Due to the overwhelming advantages offered by the Lagrangian method in terms of simplicity of formulation, ability to accommodate complicated exchange processes and computational effort, it has been adopted in the present study.

The rate of change of velocity of a discrete bubble with respect to time can be expressed as [6].

$$\frac{dV_i}{dt} = -\frac{3}{4}\frac{\mu_l}{\rho_g d_g^2} C_D R_e (V_i - U_i) + \frac{\rho_l}{\rho_g}\frac{DU_i}{Dt} - \frac{1}{2}\frac{\rho_l}{\rho_g}\left(\frac{dV_i}{dt} - \frac{DU_i}{Dt}\right) + \left(1 - \frac{\rho_l}{\rho_g}\right) g_i. \tag{7}$$

Where V_i and U_i are the instantaneous components of bubble and liquid velocities respectively in the i-direction, t is the time, ρ_g is the gas density, d_g is the bubble diameter,

$$R_e = \rho_l d_g |V - U| / \mu_l$$

is the relative Reynolds number and C_D is the drag coefficient which is empirically determined. The above equation is supplemented by the following kinematic relationship which defines the bubble trajectory

$$dx_i/dt = V_i. \tag{8}$$

The instantaneous liquid velocity is evaluated by decomposing it into a mean and a fluctuating part. The spatial distributions of the mean velocity and the r.m.s. fluctuations are obtained from the liquid phase equations. The values of the fluctuating velocities u' associated with the particular eddy that the bubble is traversing, are sampled by assuming that the fluctuations are isotropic and that these possess a Gaussian probability distribution:

$$u_i' = \phi\sqrt{\tfrac{2}{3}k} \tag{9}$$

where ϕ is a normally distributed random variable [7]. A bubble is assumed to interact with an eddy for a time equal either to the eddy lifetime

$$\tau_e = L_e/\sqrt{\tfrac{2}{3}k} \tag{10}$$

or the bubble transit time

$$\tau_t = -\tau_R \ln(1 - Le/(\tau_R |V - U|)) \tag{11}$$

whichever is the smaller [8].

Here, L_e is the eddy dissipation length scale given by

$$L_e = C_\mu^{3/4} k^{3/2}/\epsilon \tag{12}$$

and τ_R is the bubble relaxation time expressed as

$$\tau_R = \frac{4}{3} \frac{\rho_g d_g^2}{\mu_l} \frac{1}{C_D R_e}. \tag{13}$$

The above ordinary differential equations can be solved in time by simple numerical integration, starting with the given initial values. At the end of each interaction time, a new value of u_i' is sampled using Eq. (9), while u_i is updated at every time step of the integration process.

It is of course impractical to track stochastically every individual bubble released into the system, but only a statistically representative sample is needed. The residence times of bubbles in a network of control volumes superimposed on the reactor can be readily worked out from the trajectory calculations by summing the residence times of all the bubbles which pass through a given control volume ΔV and dividing by the sample size. The void fraction distribution is then obtained from

$$\alpha_g = \frac{Q}{N\Delta V} \sum_{m=1}^{n} t_{R,m}. \tag{14}$$

Where Q is the volumetric flow rate of the gas, n is the number of bubbles which pass through the control volume in question, t_R is the residence time and N is the sample size. The momentum interaction terms F_i in the liquid momentum balances are deduced from similar arguments based on the stipulation that the drag force experienced by the bubbles acts in equal magnitude but opposite direction on the liquid.

$$F_i = \frac{Q}{N\Delta V} \sum_{m=1}^{n} \int_0^{t_{R,m}} \frac{3}{4} \frac{\mu_l}{\rho_g d_g^2} C_D R_e (V_i - U_i)\, \mathrm{d}t. \tag{15}$$

The above relations can be easily generalized to take into account a spectrum of bubble sizes or gas injection from several locations.

Boundary conditions and solution procedure

The elliptic nature of the governing equations of the liquid phase requires the specification of the conditions at all the boundaries. In the regions near the solid walls the turbulence model outlined in the preceding sections does not apply. To preclude fine grid calculation the outer solutions are matched by the

empirically based log-law of the wall [9]. The values of the turbulence kinetic energy and its dissipation rate at near wall points are also deduced from wall functions. At the free surface, which is assumed to remain flat, all the stresses vanish and zero normal-gradient type conditions apply to all the dependent variables except the component of velocity normal to the surface which is zero.

The gas bubbles enter the solution domain from locations dictated by the particular configuration and at a rate determined by the gas flow rate. These are assumed to be removed from the system once they reach the free surface.

The equations to be solved are made up of 3 equations for the conservation of liquid phase momentum, the continuity equation which is transformed into an equation for pressure correction [10] and the transport equations for the turbulence kinetic energy and its dissipation rate. Coupled with these partial differential equations are the equations of motion of the bubbles which are solved to obtain the void fraction and the momentum interchange between the phases.

The finite difference grid which is superimposed onto the solution domain consists of a set of orthogonal lines in the z, r and θ directions of a cylindrical polar system of co-ordinates best suited to the geometry of the problem in hand. The usual staggered arrangement of the variables is employed where the velocity components are calculated and stored mid-way between the pressure nodes which lie at the intersections of the grid lines. The finite difference analogues of the partial differential equations are obtained by integrating these over a typical control volume which encompasses the point where the value of a particular dependent variable is to be calculated. While central differencing is used for the diffusion terms, a quadratic upstream difference scheme is employed for the convective fluxes in order to be able to minimize false diffusion problems [11].

The set of algebraic simultaneous equations thus obtained are solved iteratively by using a tri-diagonal matrix algorithm. The dependent variables are solved sequentially within each iteration and at regular intervals of the outer iteration loop, a large number of bubble trajectories are tracked stochastically to obtain the field distributions of the void fraction and the momentum exchange terms F_i. This process is continued until the equations for both phases converge to a solution.

Applications

In this section, the mathematical model is applied to the situations studied experimentally by Johansen et al. [12,13] in an air-water system. The physical ladle is shown in Fig. 1 which consists of a slightly conical perspex reactor of free surface height 1.327 m and top and bottom diameters of 1.1 m and 0.93 m respectively. Air is supplied through a porous plug which was located on the base plate, and the flow rate is varied between 1.33×10^{-4} Nm^3/s to 7.5×10^{-4} Nm^3/s.

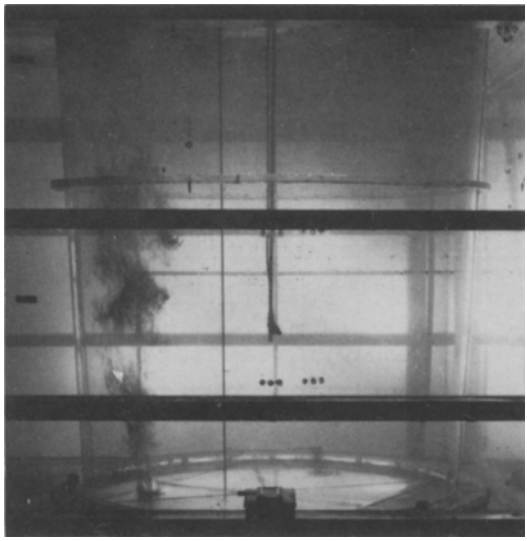

Fig. 1. The air-water model of the metallurgical ladle.

In the case where the porous plug is located centrally, the problem becomes axially symmetric and all derivatives with respect to the azimuthal direction can be neglected. The calculations in this case were carried out using a 16×16 non-uniform grid in both the axial and radial directions. The conical vessel was approximated by a cylindrical vessel of equal volume. The interphase force field and the void fraction distributions were updated at every 10 iterations of the liquid-phase solution procedure by ensemble averaging 100 stochastic bubble trajectories.

The qualitative feature of the flow field corresponding to a gas flow rate of 6.1×10^{-4} Nm^3/s are shown in the vector plot of Fig. 2. Here the vectors indicate both direction and magnitude. It can be seen that the flow has the appearance of an impinging submerged jet which, because of its entrainment appetite, gives rise to the characteristic toroidal vortex. The eye of the vortex is towards the top of the chamber and close to the vessel walls. The axial velocities are highest in the neighbourhood of the symmetry axis, while the radial velocities attain a comparable magnitude only in the vicinity of the free surface. The measured velocity vectors in the ladle are displayed in Fig. 3 which agree both qualitatively and quantitatively with the predictions.

The shape of a typical bubble column as calculated by the model is presented in Fig. 4. It can be seen that the model predicts the expected conical shape of the bubble column. The average cone angle for the range of bubble diameters between 6 mm and 12 mm was found to be around 15° which agrees fairly well with the experimental values quoted in the literature [3,4].

In addition to the above axi-symmetric calculation a simple 3-D example was also attempted. In this case, the geometry of the ladle remained unaltered

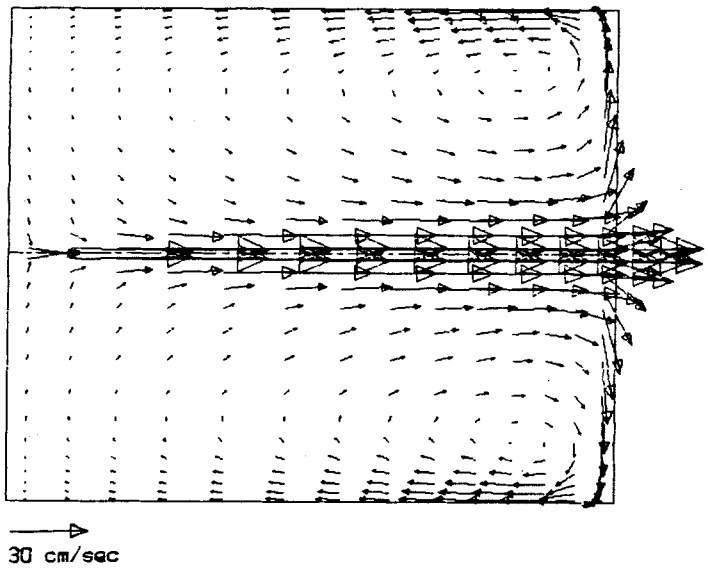

Fig. 2. Calculated velocity vectors in the ladle showing both direction and magnitude.

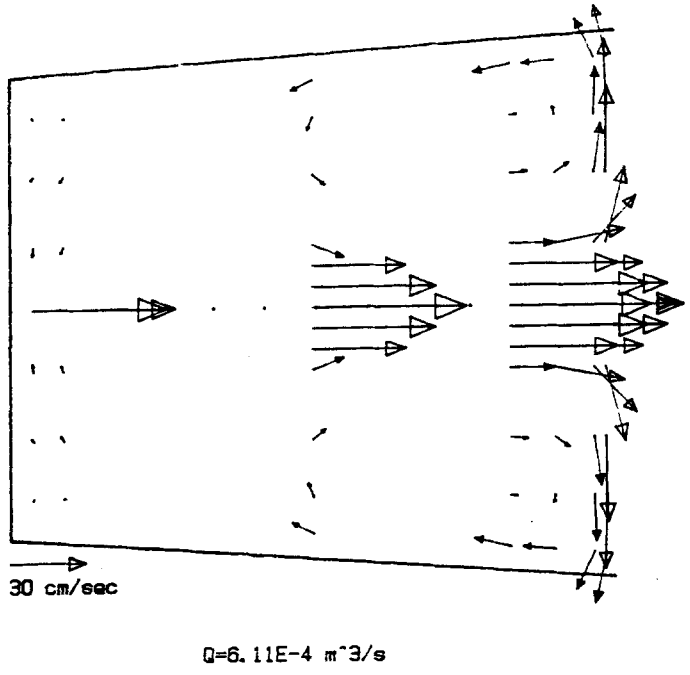

Fig. 3. Measured velocity vectors in the ladle corresponding to a gas flow rate of 6.11×10^{-4} m^3/s.

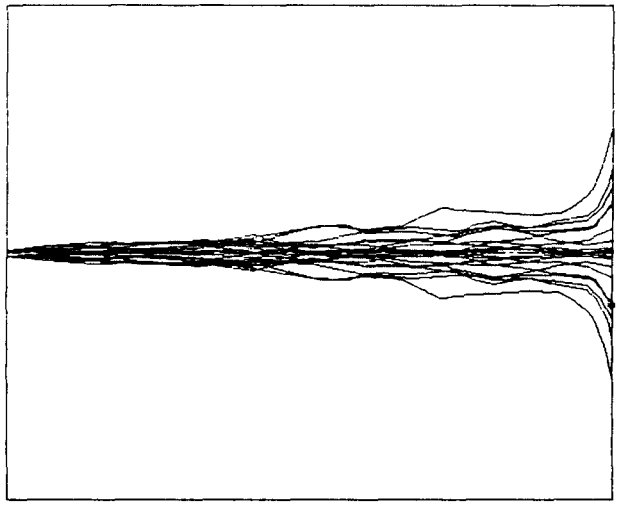

Fig. 4. Typical stochastic trajectories of 6-mm-diameter bubbles.

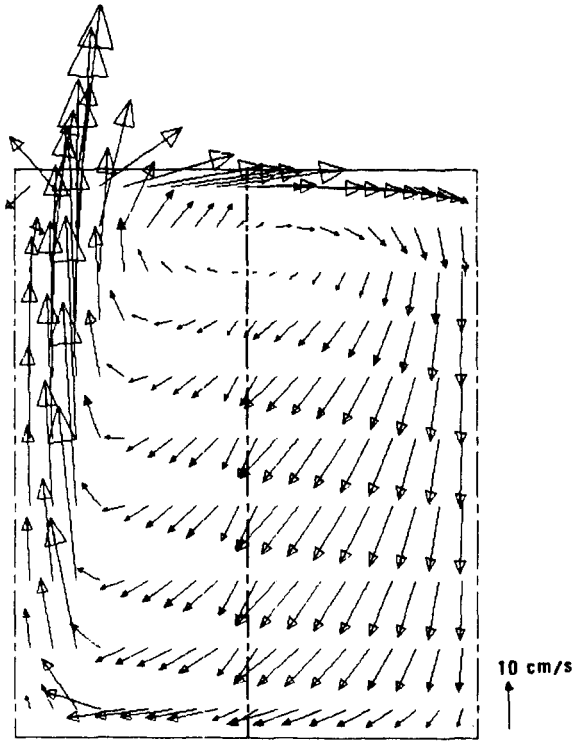

Fig. 5. Predicted velocity vectors in the case of asymmetric gas injection.

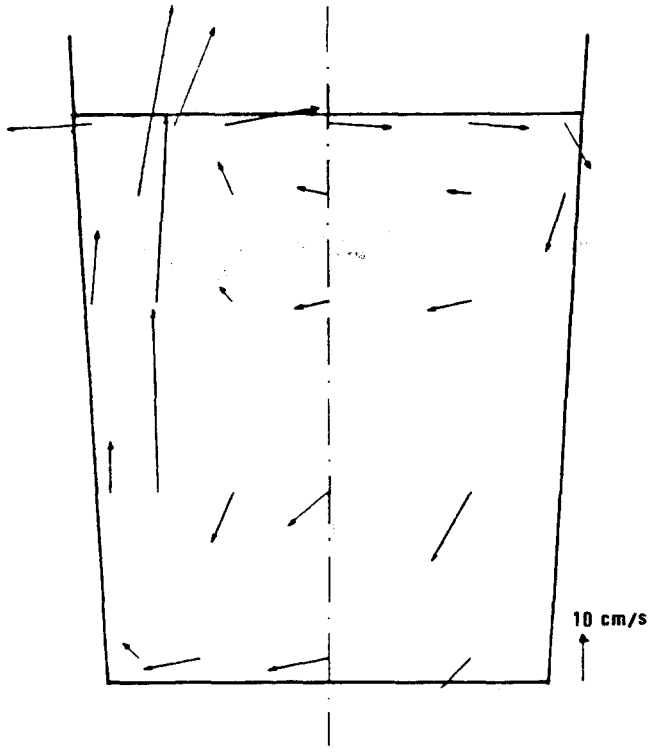

Fig. 6. Measured velocity vectors in the case of asymmetric gas injection for a gas flow rate of 5.5×10^{-4} m^3/s.

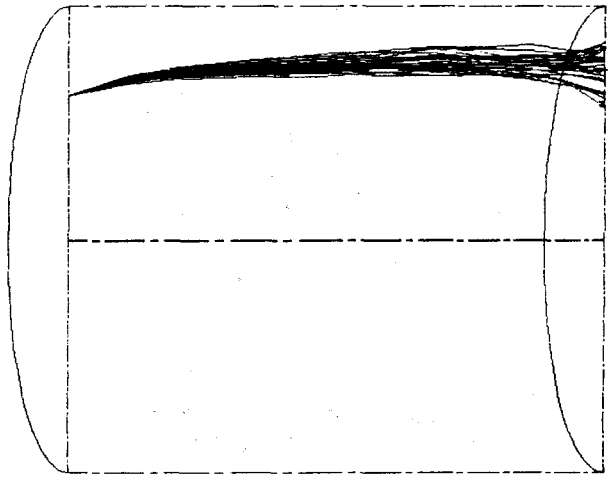

Fig. 7. Calculated trajectories of 6 mm diameter bubbles.

except that the porous plug is now moved from the axis to a position $\frac{2}{3}R$ from it. This renders the problem three dimensional. The calculations were performed on a $12 \times 12 \times 12$ grid in the z, r and Θ directions of the cylindrical polar system of coordinates. Because of the symmetry around the plane which passes through the centerline and the plug location only a 180° sector was considered in the asymmetric case. The gas flow rate was 5.5×10^{-4} Nm^3/s.

Figures 5 and 6 show the predicted and measured velocity vectors on the plane passing through the porous plug. It can be noted that in this case there is a single recirculation region the eye of which lies in the upper half of the vessel close to the free surface. The magnitude of the maximum axial velocity in this case was calculated to be 0.5 m/s which compared reasonably well with the measured value of 0.4 m/s.

The predicted shape of the bubble column is displayed in Fig. 7 which shows that it leans towards the adjacent wall and is in full agreement with experimentally observed behaviour displayed in Fig. 1.

Conclusions

A new, more fundamental approach to the mathematical modelling of gas-stirred metallurgical reactors has been described in which the complexities of the two phase bubbling jet flow have been fully addressed. By completing the mathematical picture in this way, a good degree of agreement with experimental results has been obtained, while the fundamental basis of the technique allows us a degree of confidence in applying the results to cases lying outside the compass of the experimental validations.

Work is currently underway to improve the model still further and to provide additional experimental verification under different conditions of operation.

References

1. M.J. McNallan and T.B. King: *Metallurgical Transactions B*, Vol. 13B (1982).
2. J. Szekely, H.J. Wang and K.M. Kiser: *Metallurgical Transactions B*, Vol. 7B (1976).
3. Y. Sahai and S.I.L. Guthrie: *Metallurgical Transactions B*, Vol. 13B (1982).
4. He Qinglin, Pen Yichvan and Hsiao Tse-Chiang: Shenyang Symposium of Injection Metallurgy, September (1984).
5. B.E. Launder and D.B. Spalding: *Mathematical Models of Turbulence*. Academic Press, London (1982).
6. M.R. Maxey and J.J. Riley: *Phys. Fluids* 26 (1983) 883–889.
7. A.D. Gosman and E. Ioannides: *AIAA*, paper No. 81-323 (1981).
8. J.S. Shuen, L.D. Chen and G.M. Faeth: *AICHE Journal* 29 (1983) 167–170.
9. B.E. Launder and D.B. Spalding: *Comp. Meths. Appl. Mech. Eng.* 3 (1974).
10. S.V. Patankar: *Numerical Heat Transfer and Fluid Flow*. Hemisphere, New York (1982).
11. P.G. Huang, B.E. Launder and M.A. Leschziner: UMIST Report No. TFD/83/1 (1983).
12. S.T. Johansen, D. Robertson, K. Woje and T.A. Engh: unpublished work.
13. S.T. Johansen and T.A. Engh: *Scand. J. Metallurgy* 14 (1985) 214–223.